

Decay channels and appearance sizes of doubly anionic gold and silver clusters

Constantine Yannouleas and Uzi Landman

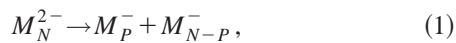
School of Physics, Georgia Institute of Technology, Atlanta, Georgia 30332-0430

(Received 7 January 2000)

Second electron affinities of Au_N and Ag_N clusters and the dissociation energies for fission of the Au_N^{2-} and Ag_N^{2-} dianions are calculated using the finite-temperature shell-correction method and allowing for triaxial deformations. Dianionic clusters with $N > 2$ are found to be energetically stable against fission, leaving electron autodetachment as the dominant decay process. The second electron affinities exhibit pronounced shell effects in excellent agreement with measured abundance spectra for Au_N^{2-} ($N < 30$), with appearance sizes $n_a^{2-}(\text{Au}) = 12$ and $n_a^{2-}(\text{Ag}) = 24$.

Unlike the case of multiply charged cationic species, the production and observation of gas-phase doubly anionic aggregates had remained for many years a challenging experimental goal. However, with the availability of large carbon clusters (which can easily accommodate the repulsion between the two excess electrons) this state of affairs changed, including observation of doubly negative fullerenes,¹ C_{60}^{2-} , and fullerene derivatives,² as well as a recent measurement of the photoelectron spectrum of the citric acid dianion.³ Moreover, such observations are not limited to carbon based aggregates and organic molecules, with a first observation of doubly anionic metal clusters (specifically gold clusters) reported^{4,5} most recently. A few theoretical studies of multiply charged anionic fullerenes^{6,7} and alkali-metal (sodium) clusters⁸ have also appeared, but overall the field of multiply anionic aggregates remains at an embryonic stage.

In this paper, we investigate the stability and decay channels of Au_N^{2-} and Ag_N^{2-} at finite temperature, and determine their appearance sizes n_a^{2-} (clusters with $N < n_a^{2-}$ are energetically unstable). Two decay channels of doubly anionic clusters need to be considered: (i) binary fission,



which has a well-known analog in the case of doubly cationic clusters,⁹⁻¹¹ and (ii) electron autodetachment via emission through a Coulombic barrier,⁸



with an analogy to proton and α decay in atomic nuclei.^{12,13} The theoretical approach we use is a finite-temperature semi-empirical shell-correction method (SCM), which incorporates triaxial shapes and which has been previously used successfully to describe the properties of neutral and cationic metal clusters.¹⁴ Our main conclusion is that, unlike the case of doubly cationic metal clusters,^{9,11} fission of Au_N^{2-} and Ag_N^{2-} is not a dominant process, and that the appearance sizes of these doubly anionic clusters are determined by electron autodetachment. Our results for the second electron affinities exhibit pronounced electronic shell effects and are in excellent agreement with the most recent experimental data⁵ for Au_N^{2-} with $n_a^{2-} = 12$. For Ag_N^{2-} , we predict $n_a^{2-} = 24$.

The finite-temperature multiple electron affinities of a cluster of N atoms of valence v (we take $v = 1$ for Au and Ag) are defined as

$$A_Z(N, \beta) = F(\beta, vN, vN + Z - 1) - F(\beta, vN, vN + Z), \quad (3)$$

where F is the free energy, $\beta = 1/k_B T$, and $Z \geq 1$ is the number of excess electrons in the cluster (e.g., the first and second affinities correspond to $Z = 1$ and $Z = 2$, respectively). To determine the free energy, we use the shell correction method. In the SCM, F is separated into a smooth liquid-drop-model (LDM) part \tilde{F}_{LDM} (varying monotonically with N), and a Strutinsky-type shell-correction term $\Delta F_{\text{sp}} = F_{\text{sp}} - \tilde{F}_{\text{sp}}$, where F_{sp} is the canonical (fixed N at a given T) free energy of the valence electrons, treated as independent single particles moving in an effective mean-field potential (approximated by a modified Nilsson Hamiltonian pertaining to triaxial cluster shapes), and \tilde{F}_{sp} is the Strutinsky-averaged free energy. The smooth \tilde{F}_{LDM} contains volume, surface, and curvature contributions, whose coefficients are determined as described in Ref. 14, with experimental values and temperature dependencies. In addition to the finite-temperature contribution due to the electronic entropy, the entropic contribution from thermal shape fluctuations is evaluated via a Boltzmann averaging.^{14(a)}

We note here that the smooth contribution $\tilde{A}_Z(N, \beta)$ to the full multiple electron affinities $A_Z(N, \beta)$ can be approximated⁸ by the LDM expression

$$\tilde{A}_Z = \tilde{A}_1 - \frac{(Z-1)e^2}{R(N) + \delta_0} = W - \frac{(Z-1 + \gamma)e^2}{R(N) + \delta_0}, \quad (4)$$

where $R(N) = r_s N^{1/3}$ is the radius of the positive background (r_s is the Wigner-Seitz radius which depends weakly on T due to volume dilation), $\gamma = 5/8$, δ_0 is an electron spillout parameter, and the work function W is assumed to be temperature independent [we take $W(\text{Au}) = 5.31$ eV and $W(\text{Ag}) = 4.26$ eV].

In a recent experiment,⁵ singly anionic gold clusters Au_N^- ($N \leq 28$) were stored in a Penning trap, size selected, and transformed into dianions, Au_N^{2-} , through irradiation by an electron beam. The measured⁵ relative intensity ratios of the dianions to their monoanionic precursors are reproduced

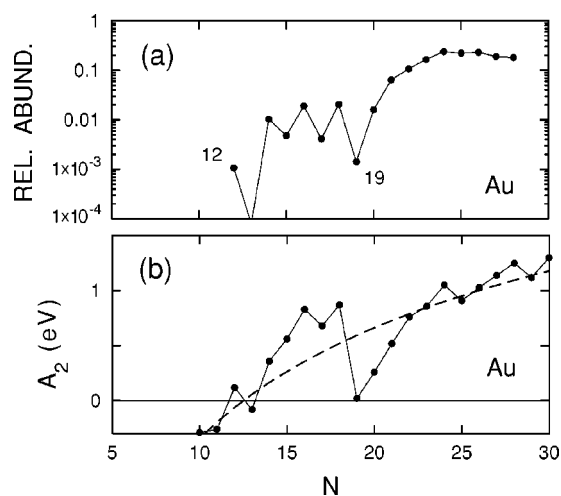


FIG. 1. (a) Measured [see Fig. 3(a) in Ref. 5] average relative abundances of Au_N^{2-} clusters (i.e., the ratio of the number of the observed dianions over the sum of the numbers of corresponding singly anionic precursors and dianions) as a function of cluster size. Note the logarithmic ordinate scaling. (b) Calculated second electron affinity (A_2 in eV) for gold clusters at $T=300$ K plotted versus N . Results from SCM calculations are connected by a solid line, and LDM results [see Eq. (4) with $Z=2$] are depicted by the dashed line. $A_2 > 0$ corresponds to stable dianionic Au_N^{2-} clusters; note the appearance size $n_a^{2-} = 12$. Energies in units of eV.

in Fig. 1(a); they exhibit size-evolutionary patterns (arising from electronic shell effects) reminiscent of those found earlier in the mass abundance spectra, ionization potentials and first electron affinities of alkali- and coinage-metal clusters.¹⁵ Since the stability of the dianions relative to their monoanionic precursors depends on the second electron affinity A_2 , it may be expected that A_2 and the relative signal intensity of the Au_N^{2-} clusters will exhibit correlated patterns as a function of size. Here we note that stable dianions must have $A_2 > 0$, whereas those with $A_2 < 0$ are unstable and decay via process (ii), i.e., via electron emission through a Coulombic barrier⁸ (see below).

In Fig. 1(b), we display the SCM theoretical results^{16,17} for the second electron affinity of Au_N clusters in the size range $10 \leq N \leq 30$. These results correlate remarkably well with the measured relative abundance spectrum [see Fig. 1(a)]. Note in particular: (i) the observed and predicted appearance size $n_a^{2-}(\text{Au}) = 12$; (ii) the relative instability of Au_{13}^{2-} [portrayed by its absence in Fig. 1(a) and the negative A_2 value in Fig. 1(b) associated with the closing of a spherical electronic subshell (containing 14 electrons) in the singly anionic Au_{13}^- parent cluster, see Ref. 14(b)]; (iii) the pronounced lower stability of Au_{19}^{2-} relative to its neighboring cluster sizes [associated with the closing of a major electronic shell (containing 20 electrons) in the Au_{19}^- parent cluster]; (iv) the overall similarity between the trends in Fig. 1(a) and Fig. 1(b) (that is, even-odd alternations for $N \leq 19$ with a sole discrepancy¹⁸ at $N=14$, or possibly at $N=15$, and the monotonic behavior for $N \geq 19$). Underlying the pattern shown in Fig. 1(b) are electronic shell effects [compare in Fig. 1(b) the shell-corrected results indicated by the solid line with the LDM curve] combined with energy-lowering shape deformations of the clusters (which are akin to Jahn-

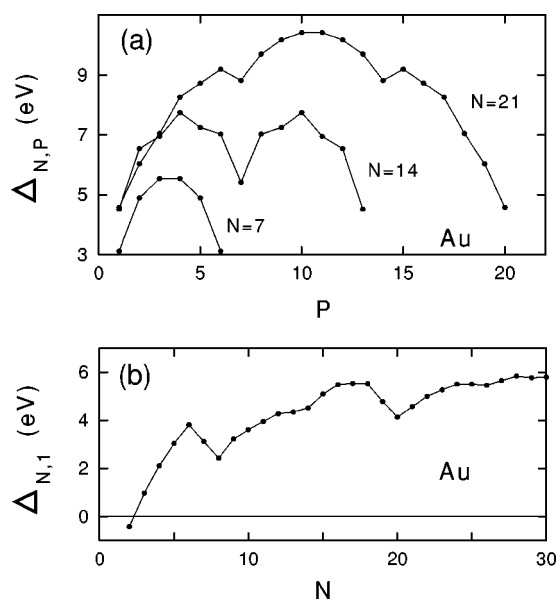


FIG. 2. (a) Fission dissociation energies ($\Delta_{N,P}$ in eV) for binary fission $\text{Au}_N^{2-} \rightarrow \text{Au}_P^- + \text{Au}_{N-P}^-$, calculated at $T=300$ K with the SCM for parent dianionic clusters with $N=7, 14$, and 21 , and plotted versus P . Note that in all cases the most favorable fission channel corresponds to $P=1$. (b) SCM fission dissociation energies, $\Delta_{N,1}$, at $T=300$ K for the most favorable channel, plotted versus cluster size. Exothermic fission ($\Delta_{N,1} < 0$) is found only for the smallest cluster.

Teller distortions and are associated with the lifting of spectral degeneracies for open-shell cluster sizes).

To explore the energetic stability of the Au_N^{2-} clusters against binary fission [see Eq. (1)], we show in Fig. 2(a) SCM results, at selected cluster sizes ($N=7, 14$, and 21), for the fission dissociation energies $\Delta_{N,P} = F(\text{Au}_P^-) + F(\text{Au}_{N-P}^-) - F(\text{Au}_N^{2-})$, with the total free energies of the parent dianion and the singly charged fission products calcu-

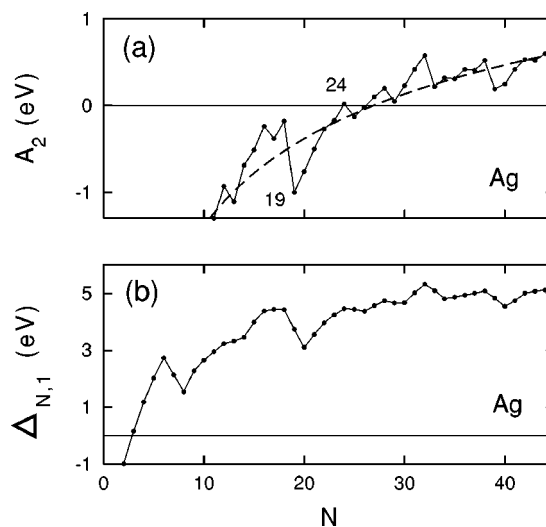


FIG. 3. SCM second electron affinities [A_2 in (a)] and fission dissociation energies [$\Delta_{N,1}$ in (b)] for the most favorable channel ($P=1$) for Ag_N^{2-} clusters at $T=300$ K, plotted versus cluster size. In (a) LDM results [see Eq. (4) with $Z=2$] are depicted by the dashed line. Note the appearance size $n_a^{2-} = 24$. Energies in units of eV.

lated at $T=300$ K. For all Au_N^{2-} parent clusters, the energetically favorable channel (lowest $\Delta_{N,P}$) corresponds to $P=1$ (i.e., one of the fission products is the closed-shell Au^- anion). The influence of shell effects on the fission dissociation energies is evident particularly in cases where the fission channel involves closed-shell magic products (see $P=7$, and equivalently $P=14$, for $N=21$, and the pronounced effect at $P=7$ for $N=14$ where both fission products are magic). The fission results summarized in Fig. 2(b) for the most favorable channel ($P=1$) illustrate that exothermic fission (that is $\Delta_{N,P}<0$) is predicted to occur only for the smallest size ($N=2$). This, together with the existence of a fission barrier, leads us to conclude that the decay of Au_N^{2-} clusters is dominated by the electron autodetachment process (which is operative when $A_2<0$ and involves tunneling through

a Coulomb barrier⁸), rather than by fission.

Finally, we show in Fig. 3 SCM results for the second electron affinity [A_2 in Fig. 3(a)] and the fission dissociation energies [$\Delta_{N,P}$ in Fig. 3(b)] corresponding to the most favorable channel ($P=1$) for silver dianionic clusters Ag_N^{2-} . Again, binary fission is seen to be endothermic except for $N=2$, and the appearance size for Ag_N^{2-} (i.e., the smallest size with $A_2>0$) is predicted to be $n_a^{2-}(\text{Ag})=24$. The shift of the appearance size to a larger value than that found for gold dianionic clusters [that is $n_a^{2-}(\text{Au})=12$, see above] can be traced to the smaller work function of silver, as can be seen from the LDM curves calculated through the use of Eq. (4) with $Z=2$.¹⁹

This research was supported by a grant from the U.S. Department of Energy (Grant No. FG05-86ER45234).

¹R.L. Hettich, R.N. Compton, and R.H. Ritchie, Phys. Rev. Lett. **67**, 1242 (1991); P.A. Limbach *et al.*, J. Am. Chem. Soc. **113**, 6795 (1991).

²C. Jin *et al.*, Phys. Rev. Lett. **73**, 2821 (1994).

³X-B. Wang, C-F. Ding, and L-S. Wang, Phys. Rev. Lett. **81**, 3351 (1998).

⁴A. Herlert *et al.*, Phys. Scr. **T80**, 200 (1999).

⁵L. Schweikhard, A. Herlert, S. Krückeberg, and M. Vogel, Philos. Mag. B **79**, 1343 (1999).

⁶C. Yannouleas and U. Landman, Chem. Phys. Lett. **217**, 175 (1994).

⁷M.R. Pederson and A.A. Quong, Phys. Rev. B **46**, 13 584 (1992).

⁸C. Yannouleas and U. Landman, Phys. Rev. B **48**, 8376 (1993); Chem. Phys. Lett. **210**, 437 (1993).

⁹C. Bréchnignac *et al.*, Comments At. Mol. Phys. **31**, 361 (1995).

¹⁰U. Näher *et al.*, Phys. Rep. **285**, 245 (1997).

¹¹C. Yannouleas, U. Landman, and R.N. Barnett, in *Metal Clusters*, edited by W. Ekardt (Wiley, New York, 1999), p. 145.

¹²S. Åberg, P.B. Semmes, and W. Nazarewicz, Phys. Rev. C **58**, 3011 (1998).

¹³M.A. Preston and R.K. Bhaduri, *Structure of the Nucleus* (Addison-Wesley, London, 1975).

¹⁴C. Yannouleas and U. Landman, (a) Phys. Rev. Lett. **78**, 1424 (1997); (b) Phys. Rev. B **51**, 1902 (1995).

¹⁵See W.A. de Heer, Rev. Mod. Phys. **65**, 611 (1993); see also Refs. 11 and 14, and references therein.

¹⁶For the rather small Au_N and Ag_N clusters discussed here ($N \leq 30$ and $N \leq 40$, respectively), our results at $T=0$ K and $T=300$ K differ only slightly. Since, however, the experiments are carried out at finite temperatures, we present here the $T=300$ K results for the sake of completeness. For cases where the SCM reveals significant thermal effects portrayed by reduction and smearing out of electronic shell effects (e.g., for higher

temperatures and/or larger r_s 's as in the case of Na_N and K_N clusters), see Ref. 14(a).

¹⁷The $T=0$ parameters entering in the SCM calculation [for definitions of these, see Ref. 14(b)] are: (i) In the case of Au_N^{Z-} clusters, $U_0 = -0.045$, $r_s = 3.01$ a.u., $t = 0.37$ a.u., $\delta_0 = 1.31$ a.u., $\delta_2 = 0$, $W = 5.31$ eV, $\alpha_v = -8.06$ eV, $\alpha_s = 2.52$ eV, and $\alpha_c = 1.04$ eV. (ii) In the case of Ag_N^{Z-} clusters, $U_0 = -0.045$, $r_s = 3.01$ a.u., $t = 0.47$ a.u., $\delta_0 = 1.31$ a.u., $\delta_2 = 0$, $W = 4.26$ eV, $\alpha_v = -8.06$ eV, $\alpha_s = 2.05$ eV, and $\alpha_c = 0.86$ eV. Experimental values were used for the liquid-drop parameters for the surface tension, α_s , and for the work function, W . α_v and δ_0 were specified through a fit to extended-Thomas-Fermi total energy calculations for spherical clusters in conjunction with a *stabilized-jellium-LDA* energy functional [see J.P. Perdew, H.Q. Tran, and E.D. Smith, Phys. Rev. B **42**, 11 627 (1990)]. The curvature coefficient, α_c , was specified by assuming that its ratio over the stabilized-jellium value is the same as the ratio between the experimental and stabilized-jellium values for the surface tension. The need to use experimental values for α_s , α_c , and W arises from the fact that the stabilized-jellium-LDA omits contributions from the d electrons and thus does not provide accurate values for the surface tension and the work function of gold and silver. The mass of the delocalized valence s electrons was taken equal to the free-electron mass. The experimental temperature dependence of the surface tension and the coefficient of linear thermal expansion were taken from standard tables as elaborated in Ref. 14(a).

¹⁸This discrepancy may be associated with the calculated value of A_2 being underestimated for $N=14$ or overestimated for $N=15$.

¹⁹The use of a finite value [see Ref. 14(b)] for the spillout parameter δ_0 in the case of negatively charged clusters is crucial for obtaining accurate results. Taking $\delta_0=0$ (as was done in Ref. 5) yields a higher value for the appearance sizes.